Thermal lens study of energy transfer in Yb^{3+}/Tm^{3+}-co-doped glasses

C. Jacinto,[1*] M. V. D. Vermelho,[1] M. T. de Araujo,[1] P. T. Udo,[2] N. G. C. Astrath,[2] A. C. Bento,[2] T. Catunda,[3] and M. L. Baesso [2]

[1] *Instituto de Física, Universidade Federal de Alagoas, 57072-970, Maceió, AL, Brazil*
[2] *Departamento de Física, Universidade Estadual de Maringá, 87020-900, Maringá, PR, Brazil*
[3] *Instituto de Física de São Carlos, Universidade de São Paulo, P.O. Box 369, São Carlos, SP, Brazil*
**Corresponding author: cjacinto@if.ufal.br*

Abstract: Energy transfer (ET) and heat generation processes in Yb^{3+}/Tm^{3+}-co-doped low-silica calcium-aluminosilicate glasses were investigated using thermal lens and photoluminescence measurements. Stepwise ET processes from Yb^{3+} to Tm^{3+}, with excitation at 0.976μm, produced efficient emission in the mid-infrared range at around 1.8μm, with high fluorescence quantum efficiency (~0.50) and relatively low thermal loading (≤0.42). An equation was deduced for the description of the thermal lens results which provided the absolute value of the ET efficiency and optimal Tm^{3+} concentration that result in population of the 1.8μm Tm^{3+} emitting level. These results suggest that the studied co-doped system would be a promising candidate for the construction of high-power diode-pumped solid-state lasers in the mid-infrared range, which are especially important for the purpose of medical procedures.

OCIS codes: (140.6810) Thermal effects; (160.3380) Laser materials; (160.4760 Optical properties.

References and links

1. L. E. Batay, A. A. Demidovich, A. N. Kuzmin, A. N. Titov, M. Mond, and S. Kuck, "Efficient tunable laser operation of diode-pumped Yb,Tm:$KY(WO_4)_2$ around 1.9 μm," Appl. Phys. B **75**, 457-461 (2002).
2. D. Y. Shen, J. K. Sahu, and W. A. Clarkson, "High-power widely tunable Tm:fibre lasers pumped by an Er,Yb co-doped fibre laser at 1.6 μm," Opt. Express **14**, 6084 (2006).
3. J. F. Wu, S. B. Jiang, T. Qua, M. Kuwata-Gonokami, and N. Peyghambarian, "2 μm lasing from highly thulium doped tellurite glass microsphere," Appl. Phys. Lett. **87**, 211118 (2005).
4. G. Galzerano, F. Cornacchia, D. Parisi, A. Toncelli, and M. Tonelli, "Widely tunable 1.94 μm Tm : BaY_2F_8 laser," Opt. Lett. **30**, 854-856 (2005).
5. S. L. Oliveira, S. M. Lima, T. Catunda, L. A. O. Nunes, J. H. Rohling, A. C. Bento, and M. L. Baesso, "High fluorescence quantum efficiency of 1.8 μm emission in Tm-doped low silica calcium aluminate glass determined by thermal lens spectrometry," Appl. Phys. Lett. **84**, 359-361 (2004).
6. C. Jacinto, D. N. Messias, A. A. Andrade, S. M. Lima, M. L. Baesso, and T. Catunda, "Thermal lens and Z-scan measurements: Thermal and optical properties of laser glasses - A review," J. Non-Cryst. Solids **352**, 3582-3597 (2006).
7. D. F. de Sousa, L. F. C. Zonetti, M. J. V. Bell, J. A. Sampaio, L. A. O. Nunes, M. L. Baesso, A. C. Bento, and L. C. M. Miranda, "On the observation of 2.8 μm emission from diode-pumped Er^{3+}- and Yb^{3+}-doped low silica calcium aluminate glasses," Appl. Phys. Lett. **74**, 908-910 (1999).
8. D. F. De Sousa, L. A. O. Nunes, J. H. Rohling, and M. L. Baesso, "Laser emission at 1077 nm in Nd^{3+}-doped calcium aluminosilicate glass," Appl. Phys. B **77**, 59-63 (2003).
9. C. J. da Silva, M. T. de Araujo, E. A. Gouveia, and A. S. Gouveia-Neto, "Fourfold output power enhancement and threshold reduction through thermal effects in an Er^{3+}/Yb^{3+}-codoped optical fiber laser excited at 1.064 μm," Opt. Lett. **24**, 1287-1289 (1999).
10. R. Scheps, "Upconversion laser processes," Prog. Quantum Electron. **20**, 271-358 (1996), and references therein.
11. Y. Jeong, P. Dupriez, J. K. Sahu, J. Nilsson, D. Y. Shen, W. A. Clarkson, and S. D. Jackson, "Power scaling of 2 μm ytterbium-sensitized thulium-doped silica fibre laser diode-pumped at 975 nm," Electron. Lett. **41**, 173-174 (2005).

#82450 - $15.00 USD Received 26 Apr 2007; revised 18 Jun 2007; accepted 3 Jul 2007; published 12 Jul 2007

12. C. Jacinto, S. L. Oliveira, L. A. O. Nunes, J. D. Myers, M. J. Myers, and T. Catunda, "Normalized lifetimes thermal lens method for the determination of luminescence quantum efficiency and thermo-optical coefficients: Application to Nd^{3+}-doped glasses," Phys. Rev. B **73**, 125107 (2006).
13. C. Jacinto, S. L. Oliveira, L. A. O. Nunes, T. Catunda, and M. J. V. Bell, "Thermal lens study of the OH^- influence on the fluorescence efficiency of Yb^{3+}-doped phosphate glasses," Appl. Phys. Lett. **86**, 071911 (2005), and references therein.
14. C. Jacinto, S. L. Oliveira, T. Catunda, A. A. Andrade, J. D. Myers, and M. J. Myers, "Upconversion effect on fluorescence quantum efficiency and heat generation in Nd^{3+}-doped materials," Opt. Express **13**, 2040-2046 (2005), and references therein.
15. J. A. Sampaio, S. Gama, M. L. Baesso, and T. Catunda, "Fluorescence quantum efficiency of Er^{3+} in low silica calcium aluminate glasses determined by mode-mismatched thermal lens spectrometry," J. Non-Cryst. Solids **351**, 1594-1602 (2005).
16. D. C. Hanna, R. M. Percival, R. G. Smart, and A. C. Tropper, "Efficient and Tunable Operation of a Tm-Doped Fiber Laser," Opt. Commun. **75**, 283-286 (1990).

1. Introduction

There has been a growing interest in the application of diode-pumped solid-state lasers that operate in the mid-infrared spectral region in several areas; such as atmospheric sensing, laser radar and medical procedures, etc [1, 2]. As a consequence of the strong optical absorption coefficient of water in this wavelength region, these devices produce minimal thermal damage to tissues, which gives them an advantage over conventional surgical procedures [1,2]. Tm^{3+} doped materials are appropriate systems for generating such laser emissions. For example, Wu *et al*. [3] developed a single-mode laser of 2 μm from a highly thulium-doped telluride-glass microsphere, and Galzerano *et al*. [4] developed a tunable laser of thulium-doped BaY_2F_8 crystal that operates at room temperature with an emission in a spectral interval of 210 nm, from 1.849 to 2.059 μm.

Recently, Oliveira *et al*. [5] demonstrated that Tm^{3+} doped Low-Silica Calcium Aluminosilicate (LSCAS) glass generates an efficient emission of around 1.8 μm when excited with a commercially available high-power diode-laser wavelength of 0.79 μm. It was also demonstrated in this paper that LSCAS samples doped with 4 or 5 wt. % Tm_2O_3 produced more efficient emissions at 1.8 μm compared to near-infrared and visible emissions at around 0.8 and 0.48 μm, respectively. Additionally, it was shown that heat generation for excitation at 1.09 and 0.79 μm was similar, despite the fact that excitation at 0.79 μm resulted in a higher quantum defect for emission at 1.8 μm. This lower heat generation was attributed to the cross-relaxation (CR) mechanisms between the doping ions [5]. These results brought new prospects for mid-infrared emission from glass matrices, because LSCAS combines the superior thermo-mechanical properties of an oxide glass with a phonon energy of the order of 800 cm^{-1}, an intermediate value compared to silicates (~1100 cm^{-1}) and non-oxide glasses (~500 cm^{-1}) [6]. These characteristics, allied to the procedure of removing the OH^- molecules from the glass structure by melting the samples under vacuum conditions, have resulted in glasses with high emission rates, as seen for (Yb^{3+}/Er^{3+}) co-doped samples with efficient emissions at 2.8 μm [7], as well as Nd^{3+} doped glasses with emissions at 1.077 μm [8]. However, several issues must be considered when Tm^{3+} doped materials are designed for efficient emission at 1.8 μm. For instance, when the concentration is increased to improve the CR mechanism and the optical absorption coefficient at the excitation wavelength, other processes arise, reducing the lifetime and thus the fluorescence quantum efficiency of the $^3F_4$-emitting level and compromising the performance of the system. For this reason, alternative schemas that can enhance emissions at 1.8 μm are desirable.

The $^3F_4$ level of Tm^{3+} can also be populated, taking advantage of energy-transfer (ET) processes by using sensitizer ions. Energy-transfer mechanisms among rare-earth (RE) ions are known to favor luminescence emission-reducing laser thresholds and to enhance amplifier gains [9]. Several materials and special glasses doped with RE ions have frequently been investigated, with the aim of using them in lasers, optical amplifiers, and frequency converters, with ET as the main mechanism [1, 5, 7, 9]. In particular, Tm^{3+} doped glasses sensitized by Yb^{3+} are recognized as efficient RE systems for obtaining laser emissions in the

#82450 - $15.00 USD Received 26 Apr 2007; revised 18 Jun 2007; accepted 3 Jul 2007; published 12 Jul 2007

visible, as well as infrared, regions [10]. Indeed, efficient tunable diode-pumped (Yb^{3+}/Tm^{3+})-co-doped-system lasers of around 2.0 μm, operating in continuous wave mode with power scaling up to 75 W, have already been developed [11]. When the medium is co-doped, the three correlated parameters, namely: optimal pump absorption, ideal concentration for optimal CR and high fluorescence quantum efficiency, can be optimized, because the limitation regarding the pump power is minimized due to the very intense optical absorption band of the sensitizer ion (Yb^{3+}) in the interval of 0.96 to 0.98 μm. Thus, the performance of the system can be strongly enhanced, if a diode-pumped laser is chosen accordingly.

The aim of this study was to evaluate the energy transfer and heat generation processes in (Yb^{3+}/Tm^{3+})-co-doped LSCAS glasses. The measurements were performed using the thermal lens (TL) and photoluminescence (PL) methods, and the focus of the study was the mechanisms responsible for the emission at around 1.8 μm. A quantitative approach to describe the generation of the thermal lens effect in the (Yb^{3+}/Tm^{3+})-system was proposed.

It is important to mention that a large number of papers are available on ET in (Yb^{3+}/Tm^{3+}) co-doped systems. However, to the best of the authors' knowledge, this is the first one to use the TL approach, which has been successfully used in the characterization of spectroscopic and thermo-optical properties of laser materials [5, 6]. In fact, it has already been applied in the evaluation of fluorescence quantum efficiency [6, 12], quenching by concentration [6, 12], OH^- impurities [13] and ET upconversion [14].

2. Experimental

The composition of the glasses studied, in wt. %, was: (41.5-x-y) % Al_2O_3, 47.4 % CaO, 7.0 % SiO_2 and 4.1 % MgO, with x = 0.5, 1.0, 1.5, 2.0 and 2.5 % Tm_2O_3 and y = 2.0 % Yb_2O_3. The samples were melted under a vacuum atmosphere, resulting in OH^- free LSCAS with IR transmittance in the order of 90 % up to 5.0 μm [15]. The photoluminescence measurements were performed in the interval between 0.4 and 2.0 μm using the excitation beam from a CW Ti:sapphire laser tuned to 0.976 μm. The TL experimental set up used is described in detail elsewhere [6]. Here, the excitation beam was also a CW Ti:sapphire laser tuned to 0.976 μm, while the probe beam was a He-Ne laser at 0.632 μm. The radiative lifetime values were calculated using the Judd-Ofelt theory for Tm^{3+} and the reciprocity method [13] for Yb^{3+} in single-doped LSCAS samples. The lifetime values were obtained from the first decay (e^{-1} decay rate) of the decay curve, using $\tau_{eff} = [\int I_{lum}(t)dt]/I_{lum}(0)$ [6,12], which is the effective lifetime, where $I_{lum}(t)$ is the decay intensity as a function of time. Indeed, a good agreement (within ~3%) between the two methods was obtained.

3. Results and discussion

Figure 1(a) shows typical luminescence spectra for the samples with 0.5 and 2.5 wt. % Tm_2O_3. It can be seen that the increase in Tm^{3+} concentration resulted in a significant enhancement in the 1.8 μm emission, compared to those at 0.48 and 0.8 μm. The fluorescence at 0.8 μm showed a small increase, while at 0.48 μm it presented a 2-fold reduction. The inset in Fig. 1(a) shows the variation of the 1.8 μm emission as a function of Tm_2O_3 concentration. This behavior can be understood with the help of the simplified energy-level diagram for Yb^{3+}/Tm^{3+}, shown in Fig. 1(b). The absorption spectrum of the Yb^{3+}/Tm^{3+}-co-doped LSCAS glass can be seen on the left-hand side. The population mechanisms for $^3F_4$, $^3H_4$ and $^1G_4$ emitting levels (not shown) occur via one (ET_1), two ($ET_1 \rightarrow ET_2$), and three ($ET_1 \rightarrow ET_2 \rightarrow {}^1F_4$) stepwise ET processes from Yb^{3+} to Tm^{3+}. The Yb^{3+} transition approximately matches the first and second ET. However, the energy mismatch, in the order of ~1900 cm^{-1}, for the third step certainly reduced the ET efficiency, as shown by the reduced 0.48 μm emission [Fig. 1(a)]. For this reason, in further analyses, this emission at 0.48 μm was ignored. Fig. 1(a) also shows the low intensity emission at 1.47 μm, ascribed to the $^3H_4 \rightarrow {}^3F_4$ transition.

When the Tm^{3+} concentration increases, the 1.8 μm emission benefits from the CR process, because of the $^3H_4, {}^3H_6 \rightarrow {}^3F_4, {}^3F_4$ transition, in which two Tm^{3+} ions interact,

#82450 - $15.00 USD Received 26 Apr 2007; revised 18 Jun 2007; accepted 3 Jul 2007; published 12 Jul 2007

resulting in two ions in the same $^3F_4$ level [depicted in Fig. 1(b)]. This process is therefore very important for Tm^{3+} lasers operating at the $^3F_4 \rightarrow {}^3H_6$ transition.

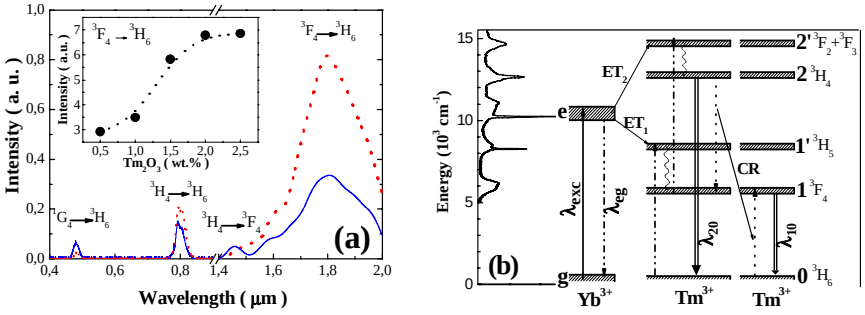

Fig. 1. (a). Photoluminescence spectra of the co-doped LSCAS glasses with 2.0 wt. % Yb_2O_3 and 0.5 wt. % (solid line) or 2.5 wt. % (dotted line) Tm_2O_3. Inset in (a): Integrated area of the 1.8 μm emission versus Tm_2O_3 concentration. (The line is a guide for the reader). (b). Simplified energy level diagram and typical optical absorption spectrum for Yb^{3+}/Tm^{3+}-co-doped LSCAS glass under excitation at 0.976 μm. The excitation and emission wavelengths (λ_{ij}) and relaxation processes are also indicated.

Table I shows the experimental and theoretical (using the Judd-Ofelt theory) fluorescence lifetime values for the $^2F_{5/2}$ level of the Yb^{3+}, as well as those for λ_{20} = 0.8 and λ_{10} = 1.8 μm Tm^{3+}, emitting levels. The lifetime values enable the evaluation of the Yb^{3+} to Tm^{3+} ET process efficiencies, as described below. When the Tm^{3+} ion concentration increases, Yb^{3+} fluorescence lifetimes decrease rapidly, indicating a very efficient ET from Yb^{3+} to Tm^{3+}. The strong reduction observed in the value of the fluorescence lifetime of the $^3H_4$ level also confirms the occurrence of the above-mentioned efficient CR mechanism. In addition, the $^3F_4$ lifetime showed a less pronounced reduction with the variation of ion concentration.

The TL technique was employed to quantify the $Yb^{3+} \rightarrow Tm^{3+}$ heat generation and ET processes as a function of Tm^{3+} concentration. The TL effect is caused by the heat generation, by means of nonradiative decay processes after laser energy absorption by the sample. In other words, the TL effect reflects the complementary part of the absorbed energy that was not converted into fluorescence. In the dual beam configuration with an excitation and a probe beam, the TL signal amplitude is proportional to the probe beam wavefront phase shift, θ, induced by the TL, generated by the excitation beam. It can be written as follows [6]:

$$\Theta = -\frac{\theta}{P_{abs}} = \left(\frac{1}{\lambda_p K}\frac{ds}{dT}\right)\varphi \qquad (1)$$

in which λ_p is the probe beam wavelength, K is the thermal conductivity, ds/dT is the temperature coefficient of the optical path length change of the sample at the probe beam wavelength, P_{abs} is the absorbed excitation power, and φ is the fractional thermal loading or the fraction of the absorbed energy that is converted into heat.

In Fig. 2(a), the squares show the fractional thermal loading (φ) and the experimental TL phase shift normalized by the absorbed pump power ($\Theta = -\theta/P_{abs}$) as a function of Tm_2O_3 concentration. As can be seen φ and thus Θ exhibit a nearly linear increase with concentration up to 1.5 wt. % Tm_2O_3, showing a saturation-like behavior beyond this concentration. Previously, φ ≈ 0.82 was obtained for the Tm^{3+}-doped LSCAS excited at either 0.79 or 1.09 μm. Therefore, the value φ ≈ 0.4 obtained for Yb^{3+}/Tm^{3+}-co-doped LSCAS glasses for the higher Tm_2O_3 concentration [shown in Fig. 2(a)] represents a significant (~100%) reduction in heat generation due to ET processes. This reduction makes the Yb^{3+}/Tm^{3+}-co-doped LSCAS glass an interesting potential system for lasers in the 1.8 μm region, mainly for high-power

#82450 - $15.00 USD Received 26 Apr 2007; revised 18 Jun 2007; accepted 3 Jul 2007; published 12 Jul 2007

diode-pumped solid-state lasers, where heat generation is very critical and can compromise the performance of the system [13,14].

Table 1. Experimental and theoretical (using the Judd-Ofelt theory) fluorescence lifetime values.

Tm_2O_3 (wt. %)	$^2F_{5/2}$ (Yb^{3+}) τ_E (ms)	$^3F_4$ (Tm^{3+}) τ_1 (ms)	$^3H_4$ (Tm^{3+}) τ_2 (ms)
0.0	1.237	-	-
0.5	0.726	3.80	0.522
1.0	0.510	3.30	0.363
1.5	0.421	3.18	0.294
2.0	0.335	3.10	0.222
2.5	0.267	2.75	0.193
τ_{RAD} (ms)	1.300	6.68	1.18

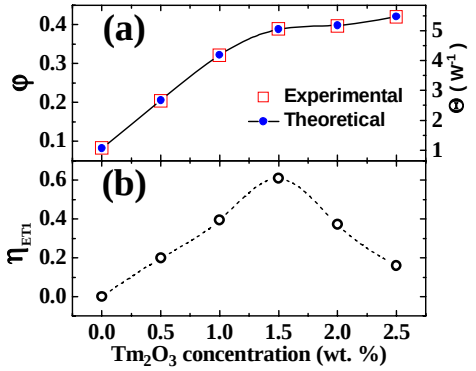

Fig. 2. (a). Experimental (squares) and theoretical (filled circles + line) thermal loading (φ) and $\Theta = -\theta/P_{abs}=13\varphi$ versus Tm_2O_3 concentration. (b) First step energy transfer quantum efficiency (η_{ET1}) versus Tm_2O_3 concentration. λ_{exc}=0.976 μm. The lines are guides for the reader.

In order to understand this behavior better, the rate equation system for the levels presented in Fig. 1(b) have been worked out, in the steady state mode. They are:

$$\dot{n}_e = R_p n_g - n_e / \tau_e \tag{2.a}$$

$$\dot{n}_1 = k_1 n_e - k_2 n_e + 2 n_2 k_{CR} + W_{21}^{mp} n_2 - n_1 / \tau_1 \tag{2.b}$$

$$\dot{n}_2 = k_2 n_e - n_2 / \tau_2 \tag{2.c}$$

in which $\tau_e^{-1} = W_e^{rad} + k_1 + k_2$ (the Yb^{3+} multiphonon decay, W_e^{mp}, was ignored due to the large energy gap for this ion) [13], $\tau_2^{-1} = W_2^{rad} + W_2^{mp} + W_2^{CR}$, $\tau_1^{-1} = W_{21}^{rad} + W_1^{mp}$, $k_1 = \gamma_1 n_o$, $k_2 = \gamma_2 n_1$, $k_{CR} = \gamma_{CR} n_o$ in which k_1, k_2 and k_{CR} are the ET probabilities for step 1, 2 and CR, respectively, and γ_1, γ_2 and γ_{CR} their respective ET parameters, and R_p is the pump rate. In order to avoid unnecessary complication, the back-transfer from Tm^{3+} to Yb^{3+} was not included. Level 1` and 2` populations were also excluded, since they decay rapidly by multiphonon to levels 1 and 2, respectively.

Generated heat, by unit of time and unit of volume, as shown in Fig. 1(b), is given by:

$$Q = R_p n_g (E_{exc} - E_{eg}) + k_1 n_e (E_{eg} - E_{1'o}) + k_2 n_e (E_{eg} - E_{21}) + W_{21}^{mp} E_{21} n_2 + W_{1o}^{mp} E_{1o} n_1 + W_{eg}^{mp} E_{eg} n_e + k_{CR} n_2 (E_{21} - E_{1o}) \tag{3}$$

#82450 - $15.00 USD Received 26 Apr 2007; revised 18 Jun 2007; accepted 3 Jul 2007; published 12 Jul 2007

In Eq. (3), W_{eg}^{mp} is negligible because of the large energy gap of the Yb^{3+} transition. Thus, this term was also not included in this equation. Heat generation, parameter φ in Eq. (1), could be evaluated from Eq. (3) through the relation $\varphi = Q/R_p n_g E_{exc}$. The resulting equation for φ is:

$$\varphi = \left(1-\eta_e \frac{\lambda_{exc}}{\lambda_{eg}}\right) - \frac{\lambda_{exc}}{\lambda_{10}}\{\eta_{ET1}[(1-\eta_1)(\eta_{CR}-\eta_2)+\eta_1]+\eta_{ET}(1-\eta_1)(\eta_2-\eta_{CR})+\eta_{CR}(\eta_{ET}-\eta_{ET1})\} - \frac{\lambda_{exc}}{\lambda_{21}}\eta_2(\eta_{ET}-\eta_{ET1}) \quad (4)$$

in which λ_{exc} = 0.976 μm, the excitation beam wavelength, and λ_{eg} = 1.02 μm, the mean Yb^{3+} emission beam wavelength. The Tm^{3+} emission wavelengths are λ_{10} = 1.8 μm and λ_{21} = 1.47 μm. η_{ET} and η_{CR} are the ET and CR efficiencies, and η_e, η_1 and η_2 are the fluorescence quantum efficiencies of the levels *e*, 1 and 2, respectively. η_{ET1} is the efficiency of the first ET, which is Tm^{3+} concentration dependent ($\eta_{ET} = \eta_{ET1} + \eta_{ET2}$). The fluorescence quantum efficiency of the level *i* can be evaluated by $\eta_i = \tau_{\exp,i}/\tau_{rad,i}$, in which $\tau_{\exp,i}$ and $\tau_{rad,i}$ are the experimental and radiative lifetimes of level *i*. Note that if $\eta_{ET} = 0$, Eq. (4) reduces to the standard φ expression of a system with only one emitting state, $\varphi = 1 - \eta\ \lambda_{exc}/\lambda_{em}$, in which λ_{em} is the average emission wavelength [6]. The ET efficiency of the CR mechanism is given by $\eta_{CR} = 1 - \tau_{\exp,2}/\tau_{o,2}$, in which $\tau_{\exp,2}$ is the experimental lifetime of the $^3H_4$ level (level 2 in Fig. 1(b)) and $\tau_{o,2}$ is the lifetime value within the limit of low Tm^{3+} concentration, for which the CR process is negligible. In addition, the ET efficiency from Yb^{3+} to Tm^{3+} can be evaluated by $\eta_{ET} = 1 - \tau_{\exp,e}/\tau_{o,e}$. All these parameters were determined using the measured lifetime values (Table 1). Therefore, the fractional thermal loading (φ) can be calculated from Eq. (4) using $\eta_{ET1}(Tm^{3+})$ as the only adjustable parameter. With φ and the constant $C = (\lambda_p K)^{-1} dS/dT = 13\ W^{-1}$, which was previously obtained in Ref. [6], Θ = C.φ can be evaluated. Fig. 2(a) presents the calculated φ values and Fig. 2(b) depicts the η_{ET1} used in these calculations versus the Tm_2O_3 concentration. As can be seen, η_{ET1} increases rapidly with Tm^{3+} concentration up to 1.5 wt. %, and thereafter, a decreasing behavior is observed. This indicates that the level emitting at 1.8 μm is efficiently excited by ET from Yb^{3+} to Tm^{3+} up to 1.5 wt. % Tm_2O_2 concentration. This highly efficient ET process can be witnessed through the reduction in the quadratic slope of the 0.8 μm emission versus pump power. This emission is due to a two-photon upconversion process populating the $^3H_4$ level, and even for low-excitation levels, its slope is still close to one (data not shown). Above the 1.5 wt. % of Tm_2O_3 concentration, the $^3F_4$ level is easily populated by CR and thus the saturation is stronger, reducing η_{ET1}. Therefore, for this Yb^{3+} concentration (2 wt. %), we can state that the optimum Tm_2O_3 content for emission at 1.8 μm is 1.5 wt. %. Another important fact was the observation that even at the higher Tm^{3+} concentration levels of these glasses, the fluorescence lifetime values (shown in Table 1), and consequently the quantum efficiency of the 1.8 μm emitting level (0.56 and 0.41 for samples doped with 0.5 and 2.5 wt. % Tm_2O_3, respectively) are much higher than those of other Tm^{3+}-doped glasses, such as for silicates, which vary from 0.06 to 0.15 [5, 16].

The results of this study show the Yb^{3+}/Tm^{3+}-co-doped LSCAS system, for laser emission in the 1.8 μm range, to be better than its corresponding Tm^{3+}-doped LSCAS system excited at ~0.8 or 1.09 μm, especially for high-power lasers, because the generated heat is greatly diminished and the 1.8 μm emitting level is efficiently excited by the ET and CR. Furthermore, other Yb^{3+} and Tm^{3+} concentrations could be analyzed in order to optimize further this co-doped system.

#82450 - $15.00 USD Received 26 Apr 2007; revised 18 Jun 2007; accepted 3 Jul 2007; published 12 Jul 2007

4. Conclusion

In conclusion, the results of this study show that the highly efficient Yb^{3+} ions transfer their energy to a less efficient Tm^{3+} ion with a thermal loading lower (100% lower for the higher Tm_2O_3 concentrations used in this work) than that for a single Tm^{3+}-doped LSCAS glass. The CR process rapidly increases with Tm^{3+} concentration and thus the $^3F_4$ level is easily populated. The equation to describe the thermal lens and luminescence data enabled the determination of the absolute values of specific ET quantum efficiency (first ET) of (Yb^{3+}-Tm^{3+}) co-doped samples, in a procedure that takes into account the main mechanisms for heat generation. Finally, the results showed that the co-doped sample with 1.5 wt. % Tm_2O_3 and 2 wt. % Yb_2O_3 was the optimal concentration studied for emission at 1.8 μm, because at these concentrations, the $^3F_4$ emitting level is efficiently populated by ET from Yb^{3+} to Tm^{3+} and by CR between Tm^{3+} ions. These results suggest that this material would be a promising candidate for the construction of mid-infrared lasers, which are especially important for the purpose of medical procedures.

Acknowledgments

The authors would like to thank the Brazilian agencies: Capes, CNPq, FAPESP, FAPEAL, FINEP, and Fundação Araucária for their financial support of this research and also Peter Grimshaw for the language revision.

#82450 - $15.00 USD Received 26 Apr 2007; revised 18 Jun 2007; accepted 3 Jul 2007; published 12 Jul 2007